

PHYSICAL AND NUMERICAL MODELLING OF SOIL-FOOTING- STRUCTURE UNDER LATERAL CYCLIC LOADING

Marios APOSTOLOU¹, Luc THOREL², George GAZETAS³, Jacques GARNIER⁴, Gérard RAULT⁵,

ABSTRACT

Rocking of stiff structures on shallow foundation has been found to enter into the nonlinear regime even under moderate seismic shaking. Post-earthquake observations of shallow foundations on stiff soils have revealed that cyclic inertial moment is often associated with large levels of transient uplift about the foundation edges. Several cases of soft soils have shown that permanent rigid-body displacements of the building (settlement, tilting) may occur, even if no prominent structural failure takes place. In the framework of the 'QUAKER' research project a series of centrifuge tests have been performed at LCPC to investigate a building with a slenderness ratio of two resting on clay under monotonic and cyclic loading. Ultimate capacity and permanent deformation of the foundation have been recorded and discussed. Nonlinear finite element modeling of the experimental tests highlights the effects of the problem parameters on the foundation response. It is shown that cyclic loading may increase the moment capacity of a foundation when compared to the static case.

Keywords: soil-structure interaction, shallow foundation, centrifuge tests, finite element modelling

INTRODUCTION

Non linear soil-structure interaction of a shallow foundation subjected to ground shaking has not yet received much attention in the geotechnical research and practice. Earthquake analysis of soil-foundation systems is often based on the assumption of linear or equivalent-linear soil behaviour and full-contact conditions between foundation and soil. However, post-earthquake observations of shallow foundations over the last decades have demonstrated that nonlinear behaviour and permanent displacements is rather inevitable during strong seismic shaking. In particular, for slender structural systems where rocking is the prevailing mode of response, nonlinear effects emerge from:

- the negligible tensile capacity of the soil-foundation interface during swaying-rocking motion, which results in uplifting of the foundation as well as in developing of second order ($P-\delta$) effects (geometrical nonlinearity),
- the plastification of the supporting soil, especially underneath the foundation edges, generated by the concentration of vertical stresses and amplified by the cyclic response of the superstructure (material nonlinearity).

¹ PhD candidate, Faculty of Civil Engineering, National Technical University, Athens, Greece, Email: m.apostolou@hol.gr

² Head of Centrifuge Modelling Group, Laboratoire Central des Ponts et Chaussées, Nantes, France.

³ Professor, Faculty of Civil Engineering, National Technical University, Athens, Greece.

⁴ Director of research, Laboratoire Central des Ponts et Chaussées, Nantes, France.

⁵ Centrifuge Modelling Group, Laboratoire Central des Ponts et Chaussées, Nantes, France.

These two mechanisms may lead to severe maximum and permanent foundation displacements (rotation and settlement) which cannot be captured by conventional, linear or equivalent linear computational methods. A series of centrifuge tests have been performed at LCPC in the framework of the EU research project 'QUAKER' to highlight the nonlinear aspects of the cyclic, dynamic response of shallow foundation. Then, non-linear finite element analysis was utilised (a) to simulate the experimental tests and (b) to carry out a fundamental sensitivity study in view of the dynamic failure envelope in the N-M plane, the dynamic (transient) foundation uplift, and the permanent vertical displacement (settlement) accumulated due to cyclic loading.

CENTRIFUGE TESTS

In this series of experiments, a 100x100 mm² footing (80x80 mm² in few cases) over soft saturated clay is submitted to (a) purely vertical, (b) monotonic horizontal and (c) cyclic horizontal loading. To this end, a servo-controlled actuator was used to operate as displacement-controlled for the static tests and force-controlled for cyclic loading. The tests were performed under a centrifugal acceleration of 100 g meaning that a scale of 1/100 should be applied to derive the prototype model. Horizontal loading is applied to the structural center of gravity at a height of 100 mm above the foundation level leading to a height-to-width ratio of two. Two values of the structural dead weight were chosen to investigate the influence of the vertical load on the rocking response. Principally, a building with a dead weight of 1284 t (for test Tub3 - T07) or 1370 t is implemented, corresponding to a heavily-loaded foundation (M1). A building with a dead weight of 580 t is also used corresponding to a lightly-loaded foundation (M2). The former gives a vertical loading ratio of $\chi = N/N_u = 0.6$ whereas for the latter it is $\chi = N/N_u = 0.26$. Soil material used in the experiments is saturated kaolin Speswhite clay at a water content of about 42 % and density of about 17 kN/m³. The total depth of the soil sample inside the container is 263 mm corresponding to a soil stratum width of 248 mm. Each container has been prepared by consolidation under stress in lab with three or four successive layers of clay. Cone Penetrometer tests were performed at 1 g before consolidation in the centrifuge, and also in-flight after reconsolidation and just before loading the structure. Shear vane tests were also carried out at several points to estimate s_u . Profiles of s_u with depth were determined using CPT and well-established correlation between q_c and s_u measured in-flight on Speswhite clay (Garnier, 2001):

$$q_c / s_u = 18.5 \quad (1)$$

Geometry and instrumentation of the model utilised at the centrifuge tests are shown in Figure 1.

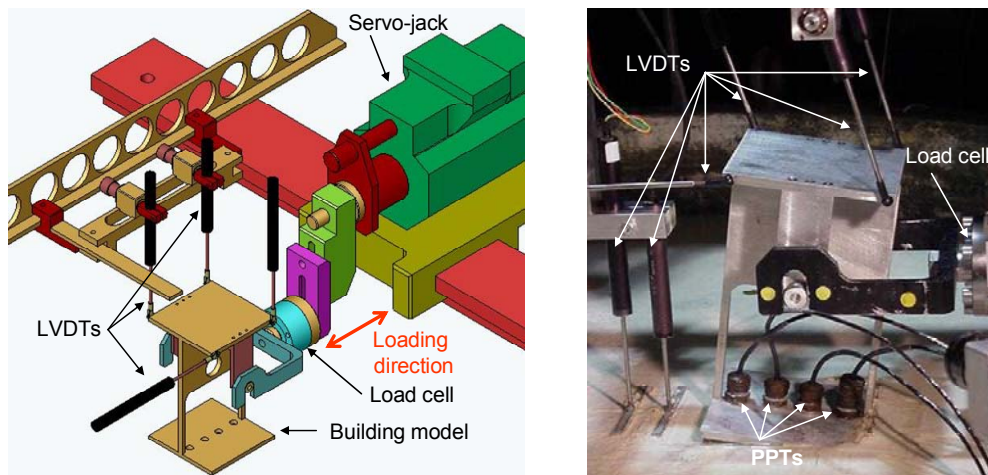


Figure 1. Loading device (left) and deformed position of model M2 after loading (right)

Loading program

Within the framework of the Quaker project the following loading conditions have been applied during the centrifuge experiments:

- Monotonic, displacement-controlled vertical loading to failure (determination of vertical bearing capacity).
- Monotonic horizontal loading to failure (with constant vertical dead weight either M1 or M2). The load is always applied at the centre of gravity, regardless of settlement or rotation.
- Cyclic horizontal loading at the gravity centre, under self weight (with and without a sand layer below the footing). The amplitude of the displacement-controlled loading is 0.4 mm (0.4 m in prototype dimensions) and the driving frequency ranges between 0.10 Hz and 0.16 Hz.

The list of the loading tests performed is presented in chronological order in Table 1 together with the values of the ultimate capacity.

Table 1. Loading program of the centrifuge tests and ultimate load

Tub n°	Test	Foundation (mm x mm)	Loading sequences	Ultimate load (MN)
Tub 1	T01	8 x 8	Vertical static (DC)	10
	T02	10 x 10	Vertical static (DC) (cancelled)	-
Tub 2	T03	8 x 8	Vertical static (DC)	16.5
	T04	10 x 10	Vertical static (DC)	24
Tub 3	T05	10 x 10	Vertical static (DC)	-
	T06	10 x 10	Vertical static (LC)	22
	T07	10 x 10 - Building M1	Horizontal static (DC)	1.4
Tub 4	T08	10 x 10 - Building M1	Horizontal static (DC)	1.2
	T09	10 x 10 - Building M1	Horizontal static (DC) Horizontal cyclic (DC)	1.3 2.0
	T10	10 x 10 - Building M1	Horizontal static (DC) Horizontal cyclic (DC)	-
Tub 5	T10	10 x 10 - Building M1	Horizontal static (DC) Horizontal cyclic (DC) Horizontal cyclic (LC)	-
	T11	10 x 10 - Building M2	Horizontal cyclic (LC)	-
Tub 6	T12	10 x 10 - Building M2	Horizontal static (DC)	0.75
	T13	10 x 10 - Building M1 (+sand layer)	Horizontal cyclic (LC)	-
Tub 7	T14	10 x 10 - Building M1	Horizontal static (DC)	-
	T15	10 x 10 - Building M2 (+sand layer)	Horizontal cyclic (LC)	-

Synopsis of test results

Prior to lateral loading, preliminary displacement-controlled tests have been performed to estimate the vertical bearing capacity of the foundation for the two structural configurations (tests T01 to T06). Due to the log-type shape of the vertical load-settlement curve no clear failure point could be identified. To overcome this, two 'conventional' failure criteria were established for settlement level of 4.5 mm and 10 mm. On the other hand, horizontal load-displacement monotonic curve after initial yielding tends to a horizontal line determining the lateral load capacity of the foundation. Ultimate loads in horizontal and vertical loading direction are presented in Table 1.

NUMERICAL SIMULATION OF CENTRIFUGE TESTS

A series of two-dimensional finite element analysis was performed to simulate the centrifuge experiments. The prototype model has been implemented in the numerical study so that all dimensions at the centrifuge model have been properly scaled up. A lumped-mass structure with a square footing ($10 \times 10 \text{ m}^2$) is considered to represent the building. The mass point located at a height of 10 m above the foundation level is connected to the foundation with a (rigid) beam element so that no flexural deformation of the superstructure is permitted. Horizontal loading is applied at this level. Rigid beam elements have been also utilised to prevent foundation mat deformations. The rigid boundary at the bottom is placed at a depth of 25 m below the foundation level. Nonlinear soil behaviour is described with a nonlinear constitutive model which incorporates the von Mises yield criterion combined with an isotropic and kinematic hardening model in the post-yield domain. This model is most suitable for the analysis of the dynamic behaviour of cohesive soils under undrained conditions. Some of the analyses were repeated by utilizing the elastic–perfectly plastic M-C model. Linear undrained strength profiles were estimated from in-flight CPT results in association with Equation (1) as presented in Table 2. These profiles have been utilised in the two-dimensional finite element analysis. The favorable effect of vertical loading to soil strength underneath the foundation has been taken into account by increasing the values of s_u at surface, up to $s_u(B/4)$. Due to lack of experimental data for the soil stiffness, Young's modulus at low deformations is considered as a linear function of the undrained shear strength. Different formulae are implemented to estimate the soil stiffness during horizontal and vertical direction.

Table 2. Linear distributions of the undrained strength with depth based on the CPT results at 100g. These values of s_u have been implemented in the finite element analysis.

Test	Undrained shear strength (kPa)	Notes
Tub1 T01	$s_u = 12.5 + 3.24z$	
Tub2 T03/T04	$s_u = 8.9 + 1.74z$	
Tub3 T06	$s_u = 18.5 + 4.24z$	Profile b
Tub3 T07	$s_u = 7.6 + 2.64z$	Profile c
Tub4 T09	$s_u = 6.4 + 3.65z$	
Tub6 T012	$s_u = 5.6 + 5.87z$	

A typical comparison of the numerical and the experimental vertical load-settlement curve (tub3 test) is presented in Figure 2. Upper and lower bound distributions of s_u from tub3 (profiles b and c respectively) have been utilized in the numerical simulation. Both numerically computed backbone curves capture the initial stiffness and the hardening behaviour (after the yield onset), of the centrifuge test. The large-displacement response and the ultimate bearing capacity calculated with profile b however are much closer to the centrifuge results. Similar trends for the vertical backbone curve are extracted from the simulation of the other tests. The experimental load-displacement curve under monotonic horizontal loading (tub3 test) is presented in Figure 3. Both profiles b and c of s_u were used for the numerical interpretation. In this case however, the soil underneath the foundation has been strengthened due to the gravitational preloading (12.6 MN). Hence, an increase of the undrained strength is considered as shown in Figure 3. A correlation of $E = 1200s_u$ was adopted for the elastic soil modulus. An excellent agreement between the experimental and the numerical results is achieved when the profile b is considered. It is also uncovered from the numerical analysis that the foundation response is marginally influenced by the contact conditions at the interface (rough or smooth). On the contrary, the ultimate horizontal load merely reaches up to 300 kN when the profile c is used; a value which is far less than the centrifuge result.

The foregoing analysis procedure was repeated with profile b, for different values of the initial load N varying from near zero to the ultimate value N_u . The horizontal load was obtained (a) at incipient yield and (b) at $u/B = 0.1$. The derived failure envelope in the N - Q space (plotted in Figure 4) can be approximated by a parabola with a local maximum at near the half of N_u . This maximum value of the shear force reaches merely 1.7 MN which is significantly lower than $As_{u0} = 2.9$ MN. The difference between the two values is attributed to the interaction in Q - M space in the former case. Furthermore, for values of N close to N_u the lateral load at $u/B = 0.1$ exceeds increasingly the yield load, due to a hardening effect.

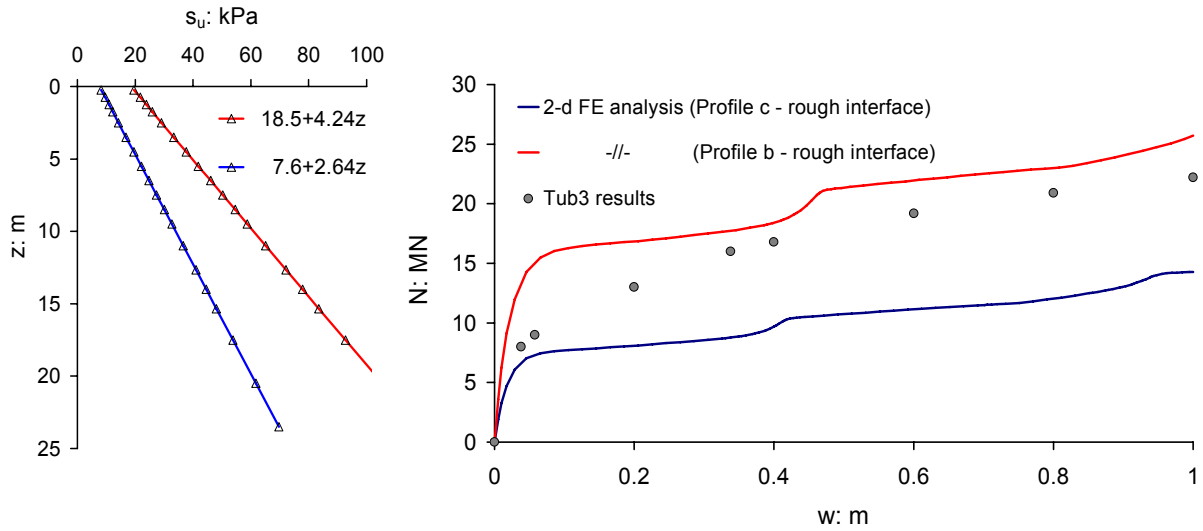


Figure 2. Monotonic vertical load-settlement curve calculated with centrifuge experiment (tub3, testT06) and comparison with the two-dimensional FE analysis

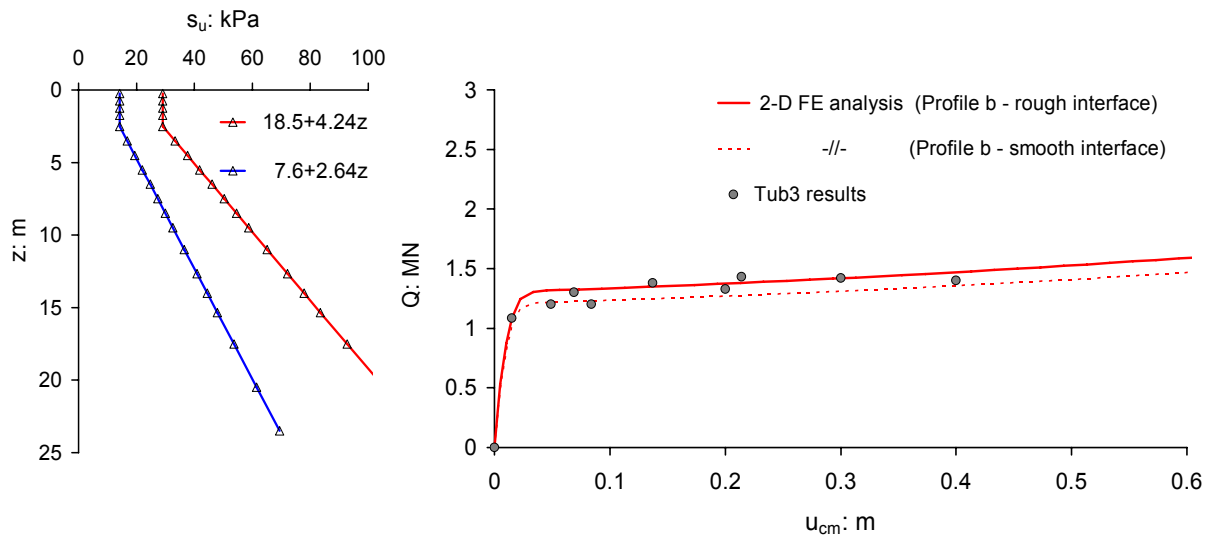


Figure 3. Monotonic lateral load-displacement curve calculated with centrifuge experiment (tub3, testT07) and comparison with the two-dimensional FE analysis

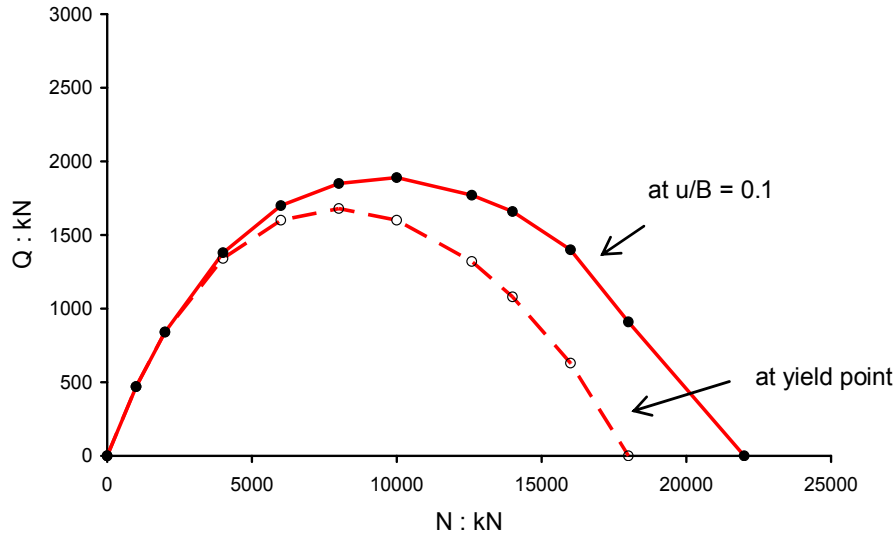


Figure 4. Monotonic failure envelope in the N-Q space calculated with two-dimensional FE analysis (tub3). For each level of vertical load, the ultimate horizontal force is calculated at incipient yield and at $u/B = 0.1$

Cyclic loading

Cyclic horizontal loading at the level of the gravity centre, under a constant vertical load was also performed in centrifuge. Typical results of the tub4 test (T09) are presented in Figure 5. Initially, a monotonic loading is applied to the structure until a prototype displacement of 0.2 m is obtained. Then the building is removed automatically to its initial position. The second (dynamic) loading phase is subdivided in three displacement-controlled cyclic sequences: (a) 10 cycles at 0.1 Hz with an amplitude of 0.4 mm (0.04 m in prototype dimensions), (b) 10 cycles at 0.16 Hz with an amplitude of 0.4 mm, and (c) 9 cycles at 0.16 Hz with an amplitude of 0.4 mm. After cyclic loading, a monotonic loading is applied to re-calculate the ultimate horizontal force. In this step the maximum force has increased from 1.2 MN to 2.1 MN which is attributed to the preceding cyclic loading. The interpretation of tub4 cyclic test is also presented in Figure 5. Finite element analysis captures both the initial and the residual (increased) shear force capacity of the foundation. Also dynamic numerical analysis provides the same maximum force with the experimental value (1.8 MN). In the numerical loops however an isotropic behaviour is revealed in the loading and unloading directions.

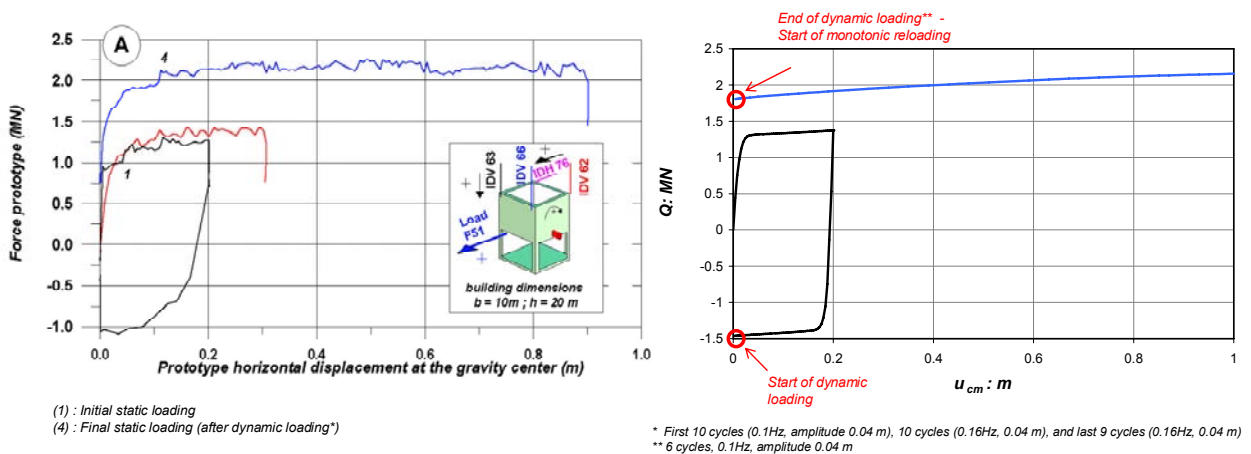


Figure 5. Backbone Q-u curves before and after cyclic loading (tub4) from the centrifuge (left) and numerical simulation (right)

FUNDAMENTAL SENSITIVITY STUDY

Nonlinear behaviour of shallow foundations subjected to earthquake loading is investigated next through a parametric finite element study.

Dynamic failure envelope N-M

A plethora of analytical studies for the calculation of interaction curves in the generalized N-M loading space has been presented by many researchers up to recently. They are all limited to the study of the problem through a static treatment (e.g. upper and lower bound solutions). However, dynamic rocking behaviour of the footing with many significant cycles may lead to substantially higher levels of the moment capacity especially for large values of the vertical load as observed in recent experiments including the QUAKEr centrifuge tests (see Figure 6).

A parametric finite element analysis has been performed in this study to elucidate the way dynamic loading affects the failure envelope of a shallow foundation. Initially, a pseudostatic approach is considered. Butterfield and Gottardi (1994) first proposed that the shape of the static failure envelope in the N-M plane for a strip footing on sand can be approximated by a parabola with a local maximum at $N = N_u/2$. Houlsby and Puzrin (1999) utilised the theorems of limit analysis to derive upper and lower bounds of the failure envelope for a cohesive (undrained) soil. The simplest analytical treatment to derive the failure envelope in the N-M plane is to represent the supporting soil with distributed elastic-perfectly plastic springs (beam-on-Winkler-foundation). A zero tensile capacity is attributed to the springs so that separation of the foundation from soil is permitted. After yield onset at an individual spring, a perfectly plastic behaviour is considered with $p = p_u$. The failure envelope in the N-M plane for the Winkler model is presented in Figure 7. In the same graph the failure envelope calculated with a non-linear push-over numerical analysis is plotted. An excellent agreement is achieved between the analytical and the finite element solution. Remarkably, for values of N close to N_u a small ‘swelling’ of the numerical curve is observed, attributed to the passive forces developed behind the footing edge.

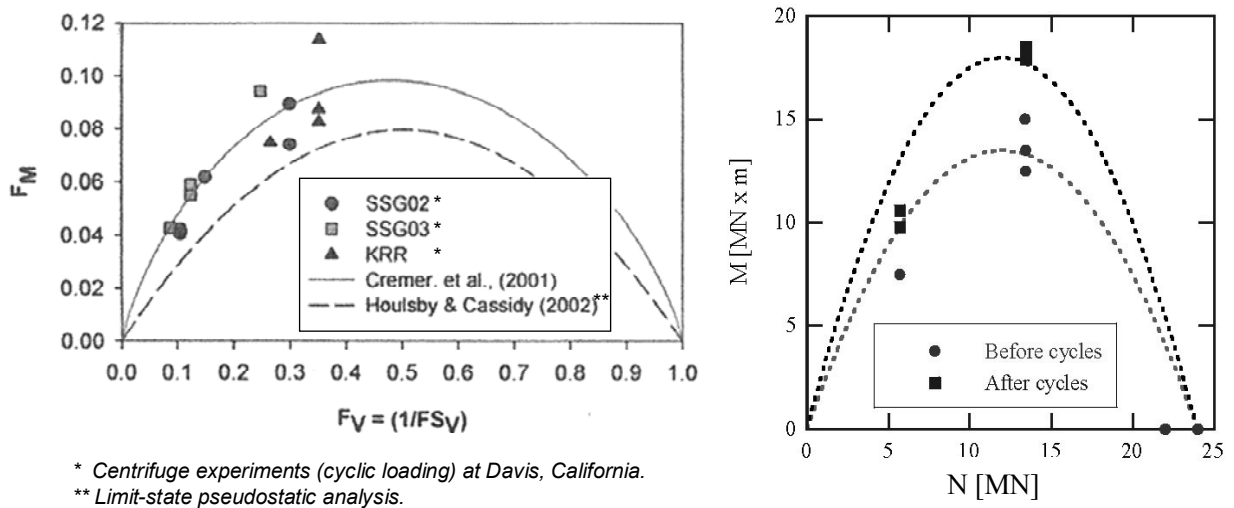


Figure 6. Failure envelope points in the N-M plane from recent experiments (left) as presented in Gajan et al. (2005) and centrifuge results from the QUAKEr project (right)

A time-domain finite element analysis series to calculate failure envelopes under dynamic loading was also performed. In this case a s-dof uplifting structure is assumed ($2b = 1$ m, $h = 5$ m) supported by a soil layer with undrained shear strength of 50 kPa. The seismic bedrock is merely at the depth of -5 m

so that any filtration of the excitation frequency content through soil is prevented ($T_s < 0.1$ sec). Despite the presence of shallow bedrock, the footing can deliberately undergo rocking oscillations as if it was supported by a half-space soil medium ($K_{R,H=5m} = 1.04K_{R,H-S}$). A Ricker pulse-type excitation is applied at the seismic bedrock with a predominant period of 0.33 sec, 0.67 sec, and 1.33 sec (Ricker nominal frequency f_R of 2.0, 1.0, and 0.5 respectively). It is considered that these values cover the period range of a typical near-fault pulse-type motion. Three levels of ground shaking have been implemented in the analysis; a weak, a moderate and a strong shaking level (PGA: 0.2 g, 0.4 g, and 0.6 g correspondingly). For each loading case the 'dynamic' moment capacity of the foundation is calculated for different values of the gravitational load N and failure envelopes in the N - M loading space are derived. Initially, the moment capacity of the footing is calculated for the short-period excitation (0.33 sec) as plotted in Figure 7. In the same graph the linear 'rigid soil' failure envelope is also presented. For the moderate and strong shaking level, a 'dynamic over-strength' is developed which is enhanced with the increase of the vertical load. Counter-intuitively, this beneficial dynamic behaviour is highly amplified close to the limiting value of $\chi = N/N_u = 1$ where the static ultimate moment approaches zero. On the other hand, for low levels of vertical load the ultimate dynamic response can be successfully predicted by the static approach or even by the 'rigid soil' linear curve ($\chi \rightarrow 0$). Only for the weak level of ground shaking the dynamic failure envelope is bounded by the static curve almost throughout the range of N . This occurs because for low levels of shaking the dynamic capacity of the foundation may not be reached. Two more Ricker wavelets with a long-duration pulse are also utilised in the study with the above-mentioned shaking levels. The resulting failure envelopes are plotted in the next two graphs of Figure 7. What is more interesting now is that the dynamic over-strength not only is even more amplified but it also approaches the 'rigid soil' moment capacity, especially for the case of $T_E = 1.33$ sec.

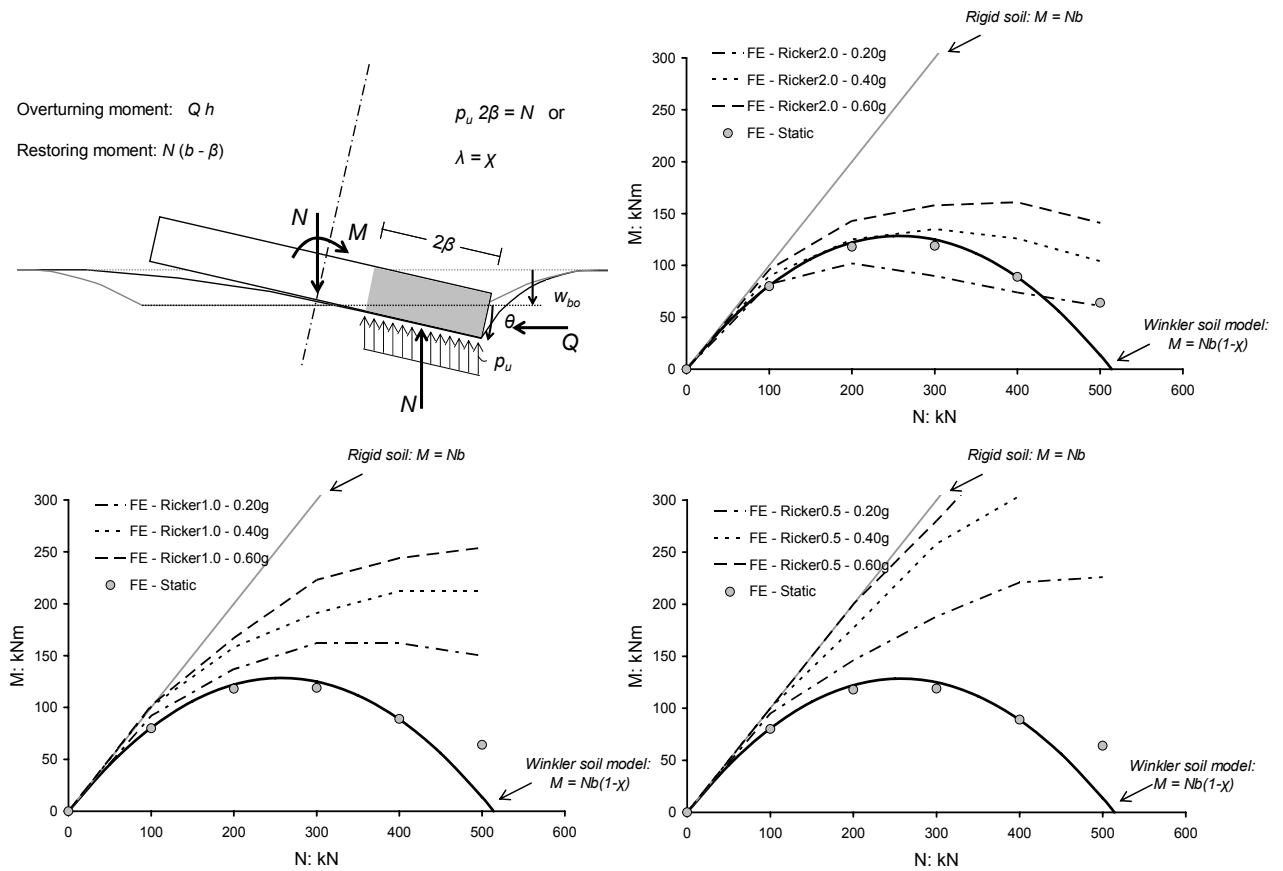


Figure 7. The simplified Winkler foundation model (top left) and the failure envelopes from static and earthquake analysis

Foundation uplift

During strong seismic shaking, rocking motion of a shallow foundation is often associated with large uplift from the supporting soil. The uplifting level is higher in case of a lightly-loaded foundation or a slender structural system. A simplified estimation for the uplifting level at static overturning conditions can be derived from the schematic of Figure 8. The supporting soil has been substituted with elastoplastic distributed springs (see Figure 7). Equilibrium of forces acting on the foundation at limit state provides that the part of the footing remaining in contact with soil is $2\beta = N / p_u$ or $\lambda = \beta / b = \chi$. A finite element validation of this approximation comes from the static results portrayed in Figure 8, for the afore-discussed soil-foundation configuration. Moreover, the earthquake-induced uplift of a shallow foundation is investigated for a Ricker-type excitation. In the next three graphs Figure 10 the ‘effective width’ 2β at $M = M_u$ is calculated from the above-discussed numerical study of the dynamic moment capacity. Depending on the frequency content of ground shaking, the dynamic interaction curve in the 2β – N plane may be located above or below the static linear trend $\lambda = \chi$. The difference of the dynamic from the static failure envelope is enlarged by the intensity of ground shaking. Hence, for a strong shaking (PGA = 0.6 g) the dynamically-induced uplift may be substantially lower ($T_E = 0.33$ sec) or higher ($T_E = 1.33$ sec) than the static prediction. On the other hand, for a weak excitation (PGA = 0.2 g) equation $\lambda = \chi$ can practically describe the uplifting level.

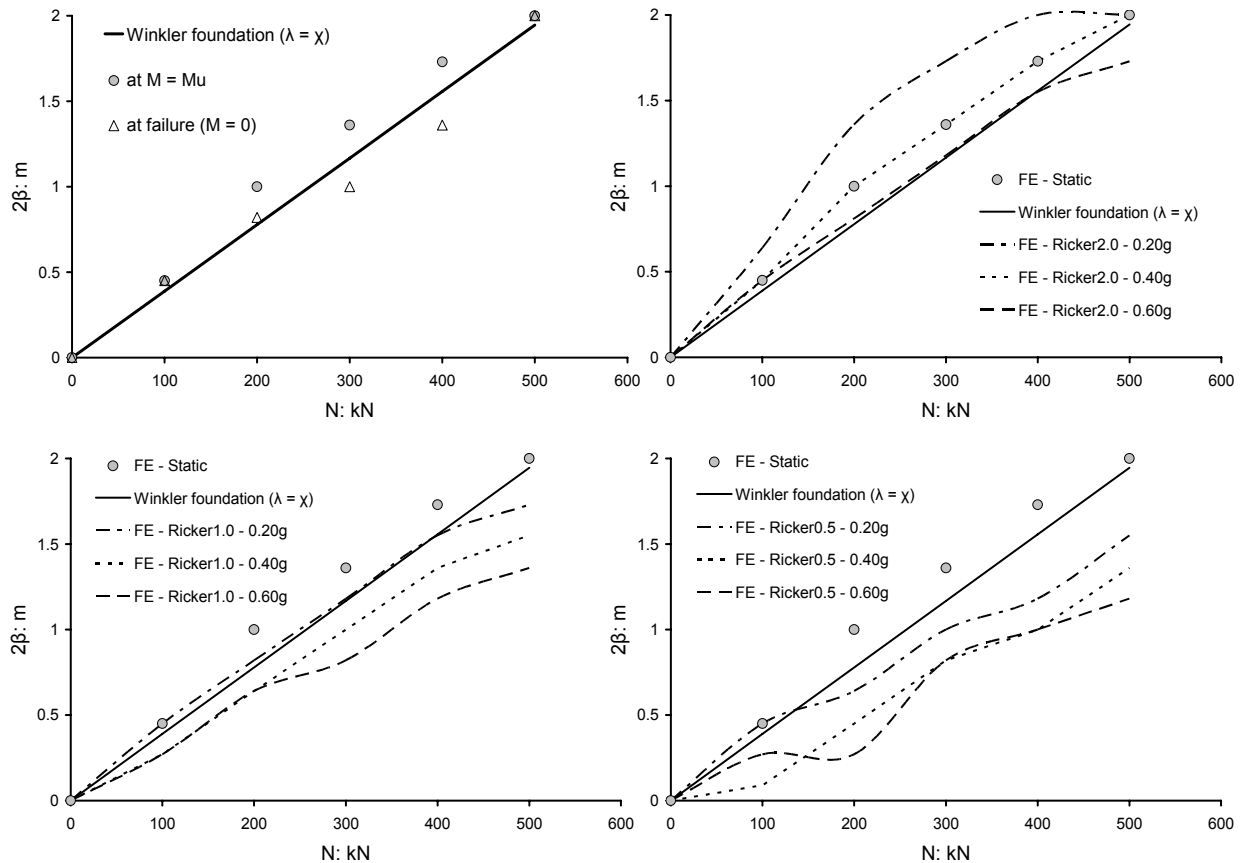


Figure 8. The numerically computed effective width under monotonic loading (a) at the increment of maximum moment (M_u), (b) at failure ($M = 0$), and comparison with the elastoplastic Winkler model. $B = 2b = 2$ m, $s_u = 50$ kPa

Permanent cyclic settlement

It has been found in the literature from both experimental and numerical studies that cyclic rocking motion of the foundation may lead to significant accumulation of permanent settlement (Gajan et al, 2004 among others). This ‘cyclic’ vertical displacement δw_{res} which is added to the initial (static) settlement w_0 is primarily sensitive to the number of cycles, the footing width, the safety factor χ , and

the frequency content of ground shaking. A parametric finite element analysis study was conducted to find estimates of the additional settlement as a function of the maximum dynamic rotation θ_{\max} . It has been shown that the cyclic settlement is very sensitive to the level of vertical loading whereas for limited levels of uplift, linear trends in the $\delta w_{\text{res}}-\theta_{\max}$ relationship may be extracted. All the numerical results are summarized in the normalised diagram of Figure 9. Similar normalised correlation between the cyclic settlement and the rocking amplitude has been recently presented in the literature extracted from a large data base of centrifuge test (Gajan, et al, 2005) as portrayed in the same figure.

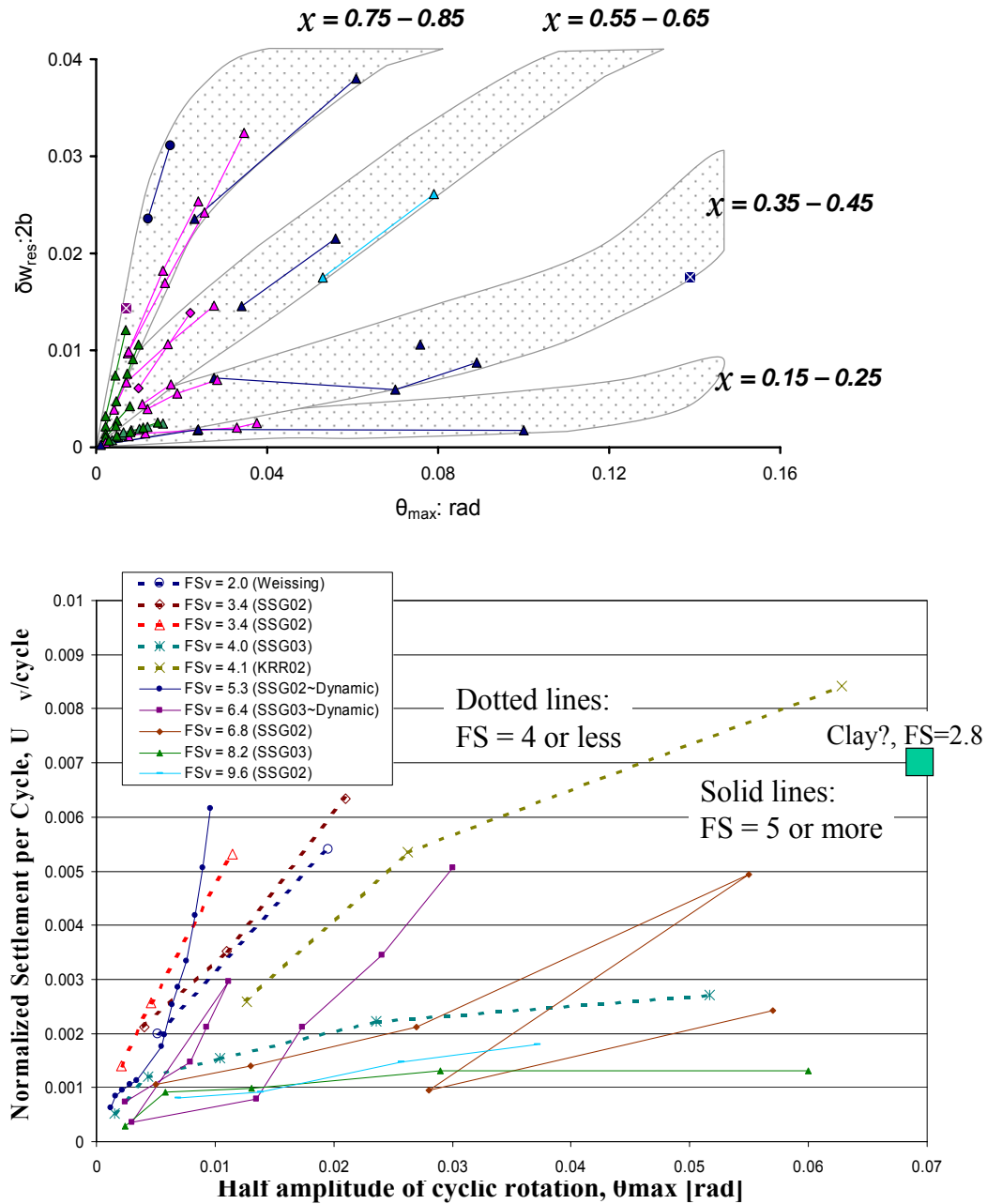


Figure 9. Normalised cyclic (additional) settlements of the foundation from (a) the present numerical study (top), (b) centrifuge experiments by Gajan et. al, 2004 (bottom)

CONCLUDING REMARKS

The most important findings drawn from the present study are as follows:

- Two-dimensional finite element analysis provides in general a very good interpretation of the centrifuge results under dynamic and cyclic loading conditions. A satisfactory agreement between plane-strain and experimental tests is also achieved.
- After cyclic loading, a slight increase of the horizontal capacity of the foundation is observed at the centrifuge and captured in the numerical simulation.
- Dynamic failure envelopes in the N-M plane may reach considerably higher levels than the corresponding static curves.
- Under monotonic loading the part of the footing remaining in contact with soil (effective width: 2β) when the moment capacity of the foundation is mobilised can be estimated by the simple relationship $\lambda = 2\beta = \chi$. This formula can be easily drawn by the footing on elastic-perfectly plastic Winkler springs model. Even under dynamic-cyclic loading conditions the effective width can be approximately calculated through this equation; however the frequency and the amplitude of the seismic excitation may be significantly different from the linear trend under certain circumstances.

ACKNOWLEDGEMENTS

The writers gratefully acknowledge the financial support received from the European Commission in terms of the research project 'Fault-Rupture and Strong Shaking Effects on the Safety of Composite Foundations and Pipeline Systems' (QUAKER), contract number: EVG1-CT-2002-00064.

REFERENCES

- Apostolou M, Gazetas G & Garini E. "Seismic response of slender rigid structures with foundation uplifting," Soil Dynamics and Earthquake Engineering, 2006 (in press).
- Bartlett P. "Foundation rocking on a clay soil," M.E. Thesis, Report No. 154, School of Eng., Univ. of Auckland, 144 pp, 1976.
- Housner G. "The behaviour of inverted pendulum structures during earthquakes" Bulletin of the Seismological Society of America, 53, No. 2, 403-417, 1963.
- Hibbitt, Karlsson, & Sorensen. "Abaqus 6.5/Standard user's manual," Hibbitt Providence, Rhode Island, 2005.
- Houlsby G. and Purzin A. "The bearing capacity of strip footing on clay under combined loading," Proc. Royal Society, 455A, 893-916, 1999.
- Butterfield R and Gottardi G. "A complete three-dimensional failure envelope for shallow footings on sand," Géotechnique 44, No. 1, 181-184, 1994.
- Gazetas G and Apostolou M. "Nonlinear soil-structure interaction: Foundation uplifting and soil yielding," 3rd UJNR Workshop on Soil-Structure-Interaction, Menlo Park, California, 2004.
- Gazetas G, Apostolou M and Anastasopoulos J. "Seismic uplifting of foundations on soft soil, with examples of Adapazari (Izmit 1999 earthquake)," International Conference on Foundations, 37-49 Dundee, Scotland, 2003.
- Gajan S, Kutter B, Phalen J, Hutchinson T and Martin G. "Centrifuge modelling of load-deformation behaviour of rocking shallow foundations," Soil Dynamics and Earthquake Engineering 25, 773-783, 2005.
- Garnier J. "Physical models in geotechnics: state-of-the-art and recent advances," 1st Coulomb Conference, Paris, 2001.
- Rault G, Thorel L and Garnier J. "Non linearity of soil-footing interaction," Quaker program, Topic B2, Progress Report No. 1, 2005.

Taiebat H. "Three dimensional liquefaction analysis of offshore foundations," PhD thesis, Univ. of Sydney, 1999.

Thorel L, Rault G, Garnier J, Escoffier S and Boura C. "Soil-footing interaction: building subjected to lateral cyclic loading," ICPMG06, 6p. (in press)

Quaker project website: www.dundee.ac.uk/civileng/quaker/index.htm.